

Fourier spectrum tensor imaging based assessment of neuronal architecture - a simulation study

Ferdinand Schweser¹, Edsel Daniel Peres Gomez¹, Andreas Deistung¹, and Jürgen R Reichenbach¹

¹Medical Physics Group, Institute of Diagnostic and Interventional Radiology I, Jena University Hospital - Friedrich Schiller University Jena, Jena, Germany

TARGET AUDIENCE – Researchers interested in MR-based quantification of tissue microstructure through phase-based Fourier spectrum tensor imaging (FTI).

PURPOSE – In a recent paper Liu and Li¹ presented a novel MR phase-based technique to assess tissue anisotropy, in the following referred to as Fourier spectrum Tensor Imaging (FTI). The technique is entirely different from both diffusion tensor imaging (DTI) and the recently introduced susceptibility tensor imaging² (STI). FTI obtains information on microstructural anisotropy, such as axonal fibers, in a certain region-of-interest (ROI; e.g. a macroscopic voxel) from the fractional Fourier spectrum that corresponds to the complex-valued MR signal of the spin ensemble inside the ROI (*Fourier sub-spectrum*)¹. The spatially resolved disentanglement of the ROI's Fourier sub-spectrum and the total k -space signal is achieved by applying physical dephasing field gradients prior to a gradient echo signal readout and then analyzing the phase of the signal average over the ROI as a function of the strength and direction of these gradients.¹ A fundamental assumption that makes FTI feasible is that the effect of the dephasing gradients can be mimicked numerically by simple k -space shifts (*shift assumption*), making the technique entirely post-processing based.¹ **With this contribution we provide important insights on the most important parameters of FTI: the MR imaging resolution, the spatial resolution of the numerical grid during the post-processing, the effect of the size of the ROI, and the sensitivity to measurement noise.**

METHODS – *Numerical model*: We created a model resembling a sample of the splenium of the corpus callosum: a cube with 4 mm side length was filled randomly with parallel axons (diameter=5 μ m; in z -direction) with intact myelin sheath ($\chi_a=-0.263$ ppm, $\chi_m=-0.1$ ppm, thickness=5 μ m) on a 5 μ m numerical grid (**Figure 1** left). The field perturbation at 9.4T (**Figure 1** right) was simulated by fast-forward field computation³ using the apparent susceptibility¹ and a magnetic field tilt of 50° relative to the axon direction¹. The field distribution was converted to a complex-valued signal at TE=20 ms assuming homogeneous magnitude. Transforming the model to k -space and discarding the Fourier coefficients exceeding a certain nominal k_{MR} mimicked MR acquisition (*MR signal matrix*). *General FTI processing*: The MR signal matrix was zero-padded to increase spatial domain resolution to a pre-defined value of Δx . Shifting the MR k -space signal by a certain vector \mathbf{p}_j ($\|\mathbf{p}_j\|_2 < \|\mathbf{k}_{MR} = [k_{MR}, k_{MR}, k_{MR}]^T\|_2$) and Fourier transforming the result simulated the effect of a dephasing gradient G_j in the spatial domain¹. The Fourier coefficient $F_{ROI}(\mathbf{p}_j)$ of the ROI's Fourier sub-spectrum was obtained by complex-valued averaging over the ROI. A flowchart of FTI processing is shown in **Figure 2**. *Dependence on MR resolution*: Using the maximum spatial resolution $\Delta x=5$ μ m (avoids spatial discretization effects) FTI processing was carried out repeatedly with MR signal matrices of different size ($1/k_{MR}$ between 5 and 157 μ m). The same 215x215x215 μ m³ ROI in the center of the FOV was used to determine all $F_{ROI}(\mathbf{p}_j)$. *Dependence on the spatial resolution of the numerical processing* (Δx): To investigate the dependence on Δx FTI was applied using $1/k_{max} = 160$ μ m, an ROI with $r = 1/k_{MR}$ and $\Delta x \cdot k_{MR}$ between 1 and 8. Due to the varying spatial resolution, Δx , the nominal matrix size of the ROI had to be adjusted for all resolutions (to maintain same effective/physical ROI size in mm; rounded integer number of voxels towards infinity). *Dependence on the size of the ROI*: To investigate the dependence on the ROI size (cube; side length r) FTI was applied using $1/k_{MR} = 360$ μ m, $\Delta x = 5$ μ m, and r between 5 and 525 μ m. *Dependence on noise*: We added white complex Gaussian noise to the MR signal with a spatial domain signal-to-noise ratio (SNR) between 1 and 400, performed FTI with 26 different shift vector directions \mathbf{p}_j and calculated the directional tensors from the resulting F_{ROI} -values¹.

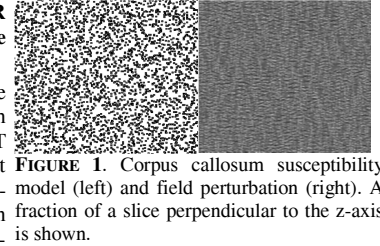


FIGURE 1. Corpus callosum susceptibility model (left) and field perturbation (right). A fraction of a slice perpendicular to the z -axis is shown.

RESULTS – **Figure 3** shows the dependence of the normalized frequency shift, i.e. $\langle F_{ROI}(\mathbf{p}_j) \rangle / \langle F_{ROI}(\mathbf{p}_{max}) \rangle$, ($\langle \cdot \rangle$ indicates the angle) as a function of the MR resolution. The relative frequency shifts (i.e., the functional dependence of $\langle F_{ROI}(\mathbf{p}_j) \rangle$) does not depend on the MR resolution. **Figure 4** shows the dependence on the spatial processing resolution (Δx). The normalized frequency shift, $\langle F_{ROI}(\mathbf{q}; [0 \ 1 \ 0]) \rangle / \langle F_{ROI}(\mathbf{q}; [1 \ 0 \ 0]) \rangle$, was independent of Δx as long as Δx exceeded 4-times the MR resolution, $1/k_{MR}$. The apparent modulation of the curves in **Figure 4** results from the slightly different regions covered by the ROIs (dotted black line; see above). **Figure 5** shows that the absolute frequency shift increases with the size of the ROI, r , and is exactly zero for $r = 5$ μ m. **Figure 6** shows the variation of tensor metrics on the MR noise level. Results imply that the directional angle and fractional anisotropy (FA) may not be evaluable precisely for SNR values below 100.

DISCUSSION – The results indicate robustness of FTI with respect to both measurement and processing parameters as long as parameters exceed certain critical values. In the original publication (Ref. 1) the relatively poor results obtained in the human brain with FTI compared to a mouse experiment indicated that the MR imaging (k_{MR}) resolution needs to be high for FTI. This said, the most important result of our current work is that FTI is independent of the MR imaging resolution (Fig. 3). Poor performance in the human brain may, consequently, be explained by FTI's high sensitivity to measurement noise (Fig. 6) and may be overcome by reducing image resolution to the benefit of SNR. Other important results of the current work is that FTI processing, first, needs to be performed on a numerical grid with relatively small voxel size (Fig. 4) and, second, larger ROIs produce higher signal (Fig. 5). Since the model in this work was highly anisotropic future studies will focus on investigating the sensitivity of the technique in the presence of partial anisotropy, e.g. in regions with crossing fibers or demyelination.

CONCLUSION – FTI is relatively insensitive to parameters of both the MR acquisition and the processing as long as the parameters exceed certain critical thresholds. In particular, FTI is independent on the MR imaging parameters.

REFERENCES – [1] Liu C and Li W, 2013. *Neuroimage*. 67:193-202. [2] Liu C, 2010. *Magn Reson Med*. 63(6):1471–7. [3] Marques JP and Bowtell RW, 2005. *Concepts Magn Reson B Magn Reson Eng*, 25B(1):65–78.

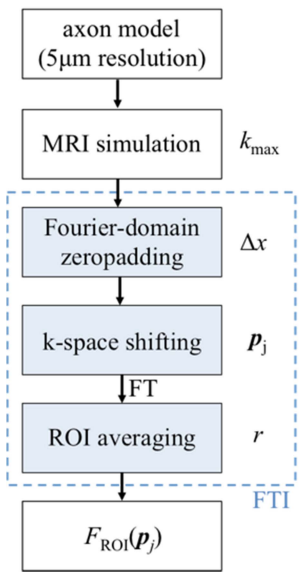


FIGURE 2. Flowchart of the FTI experiment and associated variables in the current work. The values of F_{ROI} for different \mathbf{p}_j was then used to extract anisotropy information (e.g. direction tensors).

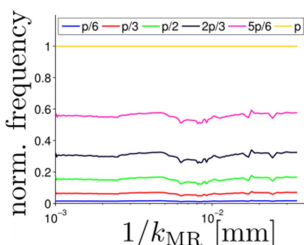


FIGURE 3. Normalized frequency for different \mathbf{p} -values over the MR imaging resolution $1/k_{MR}$.

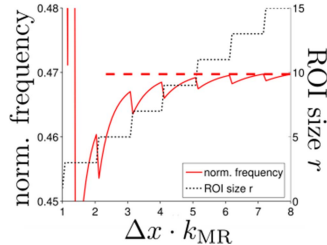


FIGURE 4. Normalized frequency (red; left y-axis) over the spatial processing resolution Δx in terms of MR imaging resolution $1/k_{MR}$. The dashed red line indicates the line of saturation for $\Delta x \cdot k_{MR} > 4$. The dotted line (black; right y-axis) shows the nominal size r of the ROI in voxels.

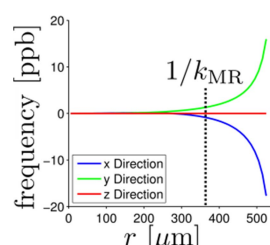


FIGURE 5. Frequency shift (in ppb) over the size of the ROI (in μ m). The dotted vertical line indicated the MR resolution used for this simulation (360 μ m).

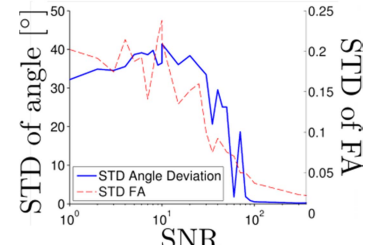


FIGURE 6. Variation of the tensor direction relative to the z -axis (blue; left axis) and variation of the tensor's FA (red, right axis) as a function of the spatial domain SNR in the MR signal.